Supporting Information

Mills et al. 10.1073/pnas.1219966110

SI Materials and Methods

The analyses presented in the main text are based on the Southwest Social Networks (SWSN) database and the associated Coalescent Communities Database (CCD) (1). The CCD is a large settlement database including size and temporal information for all known sites in the Southwest, with more than 12 rooms dating between A.D. 1200 and 1700. The SWSN Database is a spatial subset of the CCD, focused on a large portion of the Southwest west of the Continental Divide in New Mexico and Arizona, covering the period from A.D. 1200 to 1550. It is also an expansion of the CCD in that it includes frequency data on ceramic wares and types, the presence and forms of large-scale community architecture (platform mounds, great kivas, and plazas), newly verified site locations and room counts, and provenance information for obsidian objects. We defined 23 geographic subareas within the SWSN study area based on prior use in the Southwest to see how networks did or did not correspond with traditionally defined archaeological regions (Fig. 1). These subregions are based on a combination of drainage and material culture differences and are therefore not independent of the data used for network formation, but provide a way of comparing network results to past archaeological research.

The Continental Divide is a physiographic boundary but is meaningful for the study of social networks based on ceramics. During the period considered in this study, this physiographic feature falls along a relatively low population zone surrounded by densely populated areas to the east and west. The SWSN project area includes 52% of the 3,131 settlements in the CCD. Areas north of the SWSN project area that were not included in the current analyses are the northern Tusayan and Mesa Verde areas (an additional 254 settlements), both of which were completely depopulated after 1300. Areas to the south of the SWSN project area, in the states of Chihuahua and Sonora (an additional 274 sites), have sparse data for network analyses and therefore were excluded from this analysis. Such a spatial delineation of boundaries for defining social networks is also common in contemporary network analysis and is consistent with the assumptions of network theory as, unlike social groups, networks "have no natural boundaries" (2).

Ceramic Networks. In adding ceramic data, we searched published and unpublished materials (including culture resource management reports) and museum archives for information on ceramic wares and types. We also conducted analyses of museum collections and infield analyses of ceramics for sites in areas that did not have previously collected data. Our network analyses exclude "grab samples" and in most cases are from screened excavation contexts and systematically collected surface contexts such as transects or 1-m-diameter collection units. Although potential issues are raised when comparing ceramic assemblages with dramatically different sample sizes or comparing surface and excavation data, tests described below suggest that the macroregional results presented in this study are robust to these potential sources of variation.

In the Southwest, ceramic wares are defined on the basis of surface treatment (e.g., slips, pigments, texturing, polishing, smudging, and color), paste characteristics (e.g., type of aplastic materials, paste color, and texture), and when present, paint types (e.g., carbon, mineral, or glaze). Within decorated wares such as those used in this study, Southwest archaeologists distinguish among different styles of decoration and surface treatment to create a binomial taxonomy of types that changed over time within wares. Wares were produced in different geographic regions of the Southwest, some over broad areas, whereas others have more restricted distributions. Some wares have been divided into "series" that are parallel sequences of types made in different areas, such as the White Mountain Series and Zuni Series of White Mountain Red Ware. In these cases, we treated series as equivalent to wares because of the enhanced spatial control they provide. Of the 82 wares in the database, 49 are decorated (Table S1). Based on a large body of previously analyzed and reported mineralogical and chemical analyses, we estimate that 22 of the decorated wares were produced in only one subarea of the SWSN project study area. A few wares were only produced outside the study area (e.g., Rio Grande Glaze Ware). Only two wares were made in more than a few subareas: Cibola White Ware, which was made in 9 subareas and Roosevelt Red Ware (or Salado polychromes), which was made in 15 subareas. The subareas with the highest variety of locally produced decorated wares are the Puerco of the West (6 wares), Mogollon Rim (5 wares), Silver Creek (4 wares), and Zuni (4 wares). In most cases, subareas were characterized by three or fewer wares for any given time period.

The primary assumption of the methods used to construct ceramic networks here is that similarities or differences in the proportions of different kinds of ceramics can provide an indication of the strength of different kinds of relations among individual settlements and regions. For the purposes of this study, we focus exclusively on decorated ceramics as these wares typically circulated more frequently and over greater distances than undecorated ceramics in the Southwest and were more likely to consciously convey messages about status and group membership (e.g., ethnicity, polity, or religion) (3). These types were also more consistently classified across the study area than nondecorated wares. Of the 709 settlements for which we have ceramic data, we limited our sample to those 515 that have decorated ceramic counts $\geq$30 sherds (total count of 790,612 decorated sherds). For each of these 515 settlements (nodes), we then divide decorated ceramic assemblages into 50-y intervals based on the dated production ranges of each type, assumptions regarding the popularity curve for each type, and changes in population size and deposition rates through time (4).

Our chronological apportioning procedure is described in detail elsewhere (4) and is illustrated in Fig. S1. In short, for each type present at each site, we assume a standard normal curve based on the date range associated with that type and then isolate the portion of that curve that overlaps with the date range of the site in question. Next, we distribute portions of the total count of a type at the site based on the area of the popularity curve that falls within each 50-y interval. We then repeat this procedure for all types present at this site. Following this, in a step not illustrated in Fig. S1, we use the estimated growth trajectory of each site (determined based on either empirical information or an empirically based model of site growth and decline) to account for changes in site size and deposition rates through time that may influence the ceramic assemblage. Our population estimates and estimates of growth trajectories come from previously published research (1). Using this information, we apply an iterative fitting algorithm to adjust the assignment of individual sherds to each interval in which a site was occupied. Overall, this apportioning procedure is designed to allow for comparisons of assemblages from sites with different occupations spans and to minimize the effect of varying ceramic deposition rates at individual sites and variable chronological control in regional dataset.

After chronological apportioning, ceramic types were grouped into ware categories, which in the Southwest are typically long-lived, geographically cohesive, and easily distinguished sets of related ceramic types. Ceramic wares can provide an indication of

relationships among sites and regions, but are more robust to inconsistencies in recording among researchers than the finer type categories because the criteria for ware identifications are based on technological properties rather than on design style. This process allowed us to include large quantities of sherds of indeterminate type that were at least assigned to a ware category. These raw ceramic ware counts by site were converted into a matrix of similarities for each 50-y period using a similarity index ($S_{ii'}$) defined as follows:

$$S_{ii'} = 1 - \frac{\sum_j \left| \left(f_{ij}/f_{i+}\right) - \left(f_{i'j}/f_{i'+}\right) \right|}{2}$$

where $S_{ii'}$ = ceramic similarity among site i and site i'; f_{ij} = count of decorated ware j at site i; and f_{i+} = total count of all decorated ceramic wares at site i.

This similarity index ranges from 0 to 1, with higher values indicating greater similarity in site assemblages. This measure is the inverse of the commonly used index of dissimilarity and mathematically identical to the Brainerd-Robinson index of similarity often used in archaeology, rescaled to range from 0 to 1 (5, 6). The resulting similarity matrices for each 50-y interval provide a common measure of the relationships from each site to every other site in the sample in terms of the proportions of all decorated ceramic wares. We used this measure of similarity as a proxy for the strength of relationships among sites in this ceramic network. As we note in the main text, similarities in the proportions of decorated ceramics can be produced through a number of social processes including exchange, emulation, migration, and frequent interaction. At the macroregional scale that is the focus of this study, we argue that this measure of ceramic similarity combines the effects of all of these processes to provide an indication of the strongest patterned social relationships among settlements and groups of settlements (7–11).

Although our analyses were conducted using the matrix of raw similarities among sites described above, it is also useful to define binary (present/absent) ties between sites for visual display of these data. This binarization discards some of the complexity of the data as graph level and node level statistics will vary depending on the specific threshold used to define a tie. Experimentation with varying thresholds suggests that high similarity scores (~60–75% of possible similarity) provide a reliable summary of the strongest relationships among sites and regions that is consistent with the more complex representations of raw similarities among sites. For the purposes of the graphics used in this study, we defined a tie between any two sites as a ceramic similarity score of ≥0.75, but we rely on the raw, nonbinarized similarities where possible in calculating statistical measures such as eigenvector centrality.

Fig. 1 shows the binarized ties among sites with nodes positioned using the force-based Fruchterman-Reingold algorithm. This algorithm places nodes with similar sets of ties close together by creating ties that are roughly equal in length. The node sizes for each 50-y interval in this figure represent relative eigenvector centrality scores calculated based on the raw similarity matrices. Eigenvector centrality, is a measure of the overall importance or influence of a node within a network, based on the first eigenvector of the adjacency matrix, and usually calculated using binarized ties (12). Eigenvector centrality (c_i) for each node using nonbinarized similarities is similar, but individual scores are proportional to the sum of its neighbors' similarity scores rather than simply the number of binary ties:

$$c_i \propto \sum_j a_{ij} c_j$$

where c_i and c_j = eigenvector centrality scores of sites i and j, respectively, and a_{ij} = similarity score between site i and site j.

Eigenvector centrality scores are standardized such that the sum of the squared scores is equal to the total number of nodes.

Eigenvector centrality is high for a particular node when it is similar to other nodes that are also highly central. This measure is particularly relevant for the decorated ceramic data used here as eigenvector centrality takes the structure of the entire network into consideration and the measure is appropriate for network relations defined through multiple flow processes. Multiple flow processes make as few assumptions about the direction and efficiency of the flow as possible. Eigenvector centrality does not assume that relationships flow solely from node to node but rather that a node can influence all neighbors simultaneously. This conceptualization and formal definition of centrality fits well with the multiple complex processes driving relationships of ceramic similarity (e.g., exchange, emulation, cultural transmission).

Fig. 2 displays the binarized ties among all sites described above, color coded by the geodesic distances between sites. Distances were calculated between sites in a Geographic Information System (GIS) using projected Universal Transverse Mercator (UTM) coordinates (North American Datum 1927).

Assessing Sources of Variation for Ceramic Networks. As mentioned briefly in the previous section, networks created based on ceramic frequency data are subject to a number of potential influences including sampling techniques, relative sampling effort at particular sites, and the total proportion of sites included in the database. It is difficult to directly determine the effects of all of these processes, but it is possible to assess the stability of various network measures to similar perturbations using resampling (i.e., bootstrapping) methods (13).

First, to evaluate the potential impact of ceramic sample size (a function of both sampling methods and relative sampling effort) on network structure, we created a series of bootstrap replicates of the original data set for one period covered in this study (A.D. 1250–1300) with the sample sizes held constant at values of 10, 20, and 30 sherds. These sample sizes are somewhat arbitrary but are considerably lower than the mean for the period in question for the actual data (mean = 528). To create the bootstrap data sets, we resampled with replacement from the observed ware distribution for each site to create three sets of 1,000 replicates of each site ceramic assemblage, with the total sample size held constant at the three chosen intervals (10, 20, and 30 sherds for 3,000 total replicates). Each of these bootstrap data sets was then analyzed using all of the methods described above: ceramic similarity indices were produced and network centrality measures were calculated. We then produced correlation coefficients (Pearson's r) for the distributions of degree and eigenvector centrality scores between the actual data and each of the 1,000 bootstrap replicate data sets for each of the three sample sizes. We also defined binary networks using the same 0.75 cutoff for creating ties used above and calculated the absolute difference in network density. The mean correlations and density for each measure for each sample size are presented in Table S2. As this table shows, the correlations are quite high for all measures, and they also improve as the sample size increases. Mean differences in density are also small for all three sample sizes. As the above example illustrates, even with sample sizes that are considerably smaller than those represented in the actual data, broad patterns of similarity and centrality are robust to variation in ware frequency due to sample size as these patterns are primarily driven by the most common wares present. This result suggests that such patterns are also likely robust to other sources of variation in ware frequency such as differential formation processes and recovery context (e.g., surface versus subsurface), although the effects of these variables would require additional analysis.

Next, we conducted a series of bootstrap analyses designed to assess the potential effects of missing sites in our database. The

results we present here also draw on one period (A.D. 1250–1300), but we have conducted additional analyses for all periods with similar results. To simulate the effects of missing sites, we created several series of 1,000 bootstrap replicates of the original ceramic data set with varying percentages of the total site sample removed at random (25%, 50%, 75%, and 90% of the original sites removed). As in the previous example, similarity scores were produced and centrality scores calculated for each of these bootstrap replicates and calculated network density based on dichotomous ties (using the 0.75 similarity cutoff). Table S2 presents the mean correlation between actual and bootstrap data sets for degree and eigenvector centrality scores as well as the mean difference in network density (%) between actual and resampled data. As this table shows, mean correlations for centrality measures are all high, even when as many as 90% of the sites in the original sample are removed. Further, the largest mean difference in network density is only about 1.6% even when 90% of sites are removed. Overall, these results suggest that the distributions of centrality scores and density are both extremely robust to the inclusion or exclusion of specific sites. This suggests that the results presented here are unlikely to be influenced substantially by the absence of sites where ceramic data were not available.

Spatial Analyses. To explore the role of geography in promoting or constraining networks of interaction across our study area, we defined a measure of spatial connectivity among sites based on settlement location, site density, and terrain. The settlement data used for this portion of the study are derived from the CCD (1), which contains room counts and date ranges for all available sites of 13 rooms or more (ca. A.D. 1200–1700) within our study area and beyond. This database includes all known late pre-Hispanic sites, even those for which we do not have ceramic or obsidian data. During the interval considered here, much of the population of the Southwest resided in relatively large settlements, so this database likely contains the vast majority of residential settlements.

Because the spaces between settlements in our study area are dissected by numerous mountain ranges, valleys, and canyons, it is necessary to take terrain into account when assessing distances among sites. Here we use GIS methods for least cost analysis to take costs of travel in terms of energy expenditure into consideration. In this study, we use a simple travel cost model, described in detail elsewhere (14), based simply on slope (calculated based on a 30-m resolution digital elevation model), as well as the average weight and leg length of an individual. We do not argue that these results reconstruct the specific paths that would have been used in the past, but they do provide a better indication of the relative distances between sites than linear distances alone.

Our approach differs from traditional site catchment analyses in at least one important way; rather than characterizing local resources in the natural environment it focuses on social resources indicated by the proximity of other people with whom to engage in socially networked activities. A significant result of this distinction is that such network activities have the potential to link communities across large areas. Thus, sites may become part of linked groups connected by knowledge and information more easily across much greater distances than is logistically practical for many material resources.

To develop a measure of cost-adjusted proximity among all sites, we created a friction surface (a surface indicating the relative costs associated with travel in any direction) around all sites occupied during each 50-y interval. Fig. S2 displays all cost-adjusted buffers color coded by this measure of connectivity. We argue that this measure provides an indication of potential social connections among settlements as areas with a higher local site density across shorter distances might be expected to be areas with higher network density as expressed through other lines of material evidence. Fig. S3 then shows the proportions of possible ties (i.e., density) among sites within overlapping 9-km cost-adjusted buffers and among sites in different buffers by time period for the northern vs. the southern Southwest. As these plots illustrate, such binarized ties are consistently more frequent for sites in the same buffer, but these differences diminish considerably for the A.D. 1350–1400 and A.D. 1400–1450 intervals in the southern Southwest. This result suggests that spatial proximity may have had less influence on strong connections in the south during the last few generations of the major pre-Hispanic occupation of the region.

Using these cost-adjusted site buffers, it is also possible to assess the degree to which material cultural similarities (ceramics and obsidian) are influenced by the spatial concentration of sites. Our basic assumption is that settlements within a common set of overlapping cost-adjusted buffers likely shared land use catchments and thus, we would expect a considerably greater degree of interaction and ceramic/obsidian similarity among settlements with overlapping buffers if patterns of similarity were strongly influenced by geography. For the purposes of this analysis, we used 9-km cost-adjusted buffers as a proxy for local connections as these buffers represent distances that could be traversed between sites, out and back, within half a day of travel (14). To assess the relationship between spatial concentration and ceramic similarity, we calculated the distribution of similarity scores among sites within overlapping 9-km buffers and then calculated similarity scores among sites that did not share overlapping 9-km buffers for each time period. We then compared similarity scores within and between buffers using a one-sided, nonparametric Mann–Whitney U test to assess the probability that sites within buffers had greater ceramic similarity than sites not in the same buffer.

As Table S3 shows, for all time periods, ceramic similarity scores were statistically significantly greater for sites within the same buffers than for sites in different buffers. However, the total difference in mean similarity scores for connections within and between buffers also decreases through time. Overall, this analysis suggests that the spatial distribution of sites does play a major role in the strength of social connections among sites, but the strength of this relationship diminishes through time. Moreover, as brought out in the main text, the ability of spatial distance to predict social connectivity in terms of degree centrality is low.

Obsidian Networks. Approximately 30 obsidian sources were commonly used by the pre-Hispanic inhabitants of the Southwest, and a unique trace element fingerprint has been established for each. We consider 11 major sources that were determined empirically to be used extensively within our study area. These sources vary considerably in nodule size and workability, as well as abundance that may have influenced preference to some extent. However, all frequently used sources are associated with ample quantities of workable obsidian nodules at least 5 cm in length. These nodules would have been easy to transport by foot and of sufficient size to produce the small projectile points for which they were almost exclusively used (15). At the large scale used in this paper, we assume that proximity and social factors were more important than small differences in quality in the procurement and exchange of these 11 commonly used sources.

We characterize obsidian procurement and exchange patterns using a large database of obsidian artifacts whose source determinations have been made using X-ray fluorescence (XRF). Our total sample includes more than 4,800 sourced artifacts from 140 late pre-Hispanic sites distributed throughout the project area (Tables S4 and S5). For a variety of factors, including where large cultural resource management projects have been conducted over the last 50 y, more sites with sourced obsidian are present in the southern portion of the project area than the northern portion. To determine where and when patterns of obsidian procurement differ from what we might expect based on geography alone, we

also developed a null model of obsidian procurement based on the cost-adjusted travel costs from each site to the nearest point it intersected the perimeter of the primary deposit of each major source (some of these deposits are extensive, covering many square kilometers). Secondary deposition of several sources in streambeds (e.g., Cow Canyon, Mule Creek) is well known, but poorly defined on the ground, so only primary deposits are considered here. However, we present only robust patterns in this paper that may be attenuated by procurement of secondarily deposited obsidian, but not negated.

Travel costs were estimated using the methods described in the previous section from each site with obsidian data to the perimeter of the 11 most intensively used obsidian sources, which account for more than 99% of all sourced samples. The relative travel costs from each of the 11 sources to each site were then used to create an expected obsidian distribution for each site where geography was the only consideration. Sites within a 1-d round trip from an obsidian source (18 cost-adjusted K_m each way) were expected to have only that local source. Sources greater than an estimated 10 d of travel from a site (>360 cost-adjusted K_m) were considered to have no contribution. For the remaining nonlocal sources, obsidian source use was assumed to follow a distance decay inverse power law relationship. Using this function, expected proportional distance decay source assemblages were calculated for each site:

$$P_i = \frac{\left(1/d_i^2\right)}{\sum_j \left(1/d_j^2\right)}$$

where P_i = expected relative proportion of obsidian source i; d_i = cost-adjusted distance from the nearest point of obsidian source i to site; and j = all nonlocal obsidian sources <360 cost-adjusted K_m from site.

To determine which sites deviated from expected proportions, we simulated 1,000 obsidian samples for each site using the proportions determined by the above distance decay formula as a multinomial probability distribution and with the sample size equal to the actual sample for each site. We then calculated similarities between the proportions of sources represented in each actual assemblage and the expected assemblage based on the distance decay model using the measure of similarity described for ceramic networks above ($S_{ii'}$) ranging from 0 to 1 (with 1 equal to perfect similarity). Finally, we then calculated similarities between each of the 1,000 simulated assemblages for each site and the expected distance decay assemblage. Sites were defined as deviating from the distance decay expectation when the mean similarity score for the simulated assemblages was at least 2 SDs greater than the similarity score between the actual and expected assemblage. For sites that deviated from distance decay, the expected proportions of sourced obsidian artifacts were then subtracted from the actual proportions to determine which sources were over- or underrepresented and by how much. Over- and underrepresentation was divided into three categories: low, moderate, and high at minimum thresholds of 10%, 30%, and 50% more or less than expected. Fig. 4 shows the results of this procedure.

Finally, we compared ceramic similarities among sites that shared a common source overrepresentation with all sites with obsidian and ceramic data in our sample for the pre- and post-A.D. 1300 intervals. Table S6 shows the mean ceramic similarity for all sites that share an overrepresentation of a given source compared with the mean similarity for all other sites with obsidian. The third column shows probabilities based on one-sided, nonparametric Mann–Whitney U tests comparing the distribution of ceramic similarity scores for sites in which a particular source is overrepresented against those in which it is not. As described in the main text, before A.D. 1300, only sites that share an overrepresentation of the Jemez source have significantly higher ceramic similarity scores than those that do not share an overrepresentation of the Jemez source. After A.D. 1300, with the exception of the San Francisco Volcanics, sites that share a common overrepresentation of a specific source have significantly higher ceramic similarity scores than sites that do not share an overrepresentation of a specific source.

1. Hill JB, Clark JJ, Doelle WH, Lyons PD (2004) Prehistoric demography in the Southwest: Migration, coalescence, and Hohokam population decline. *Am Antiq* 69(4):689–716.
2. Borgatti S, Halgin DS (2011) On network theory. *Organizational Science* 22(5):1168–1181.
3. Mills BJ, Crown PL, eds (1995) *Ceramic Production in the American Southwest* (Univ of Arizona Press, Tucson, AZ).
4. Roberts JM, Jr., et al. (2012) A method for chronological-apportioning of ceramic assemblages. *J Archaeol Sci* 39(5):1513–1520.
5. Brainerd GW (1951) The place of chronological ordering in archaeological analysis. *Am Antiq* 16:301–313.
6. Robinson WS (1951) A method for chronologically ordering archaeological deposits. *Am Antiq* 16:293–301.
7. Duff AI (2002) *Western Pueblo Identities: Regional Interaction, Migration, and Transformation* (Univ of Arizona Press, Tucson, AZ).
8. Nelson MC, Kulow S, Peeples MA, Hegmon M, Kinzig A (2011) Resisting diversity in small scale societies: A long-term archaeological study. *Ecol Society* 16(1):article 25.
9. Rautman AE (1993) Resource variability, risk, and the structure of social networks: An example from the prehistoric Southwest. *Am Antiq* 58(3):403–424.
10. Adams EC, Duff AI, eds (2006) *The Protohistoric Pueblo World, A.D. 1275-1600* (Univ of Arizona Press, Tucson, AZ), pp 137–143.
11. Peeples MA (2011) Identity and social transformation across the prehispanic Cibola World: A.D. 1150-1325. PhD dissertation (Arizona State Univ, Tempe, AZ).
12. Wasserman S, Faust K (1997) *Social Network Analysis: Methods and Applications* (Cambridge Univ Press, New York, NY).
13. Mills BJ, et al. (2013) *New Approaches in Regional Network Analysis*, eds Knappett C, Rivers R (Oxford Univ Press, New York, NY).
14. Herhahn C, Hill B (1998) Modeling agricultural production strategies in the northern Rio Grande Valley, New Mexico. *Hum Ecol* 26:469–487.
15. Shackley MS (2005) *Obsidian: Geology and Archaeology in the North American Southwest* (Univ of Arizona Press, Tucson, AZ).

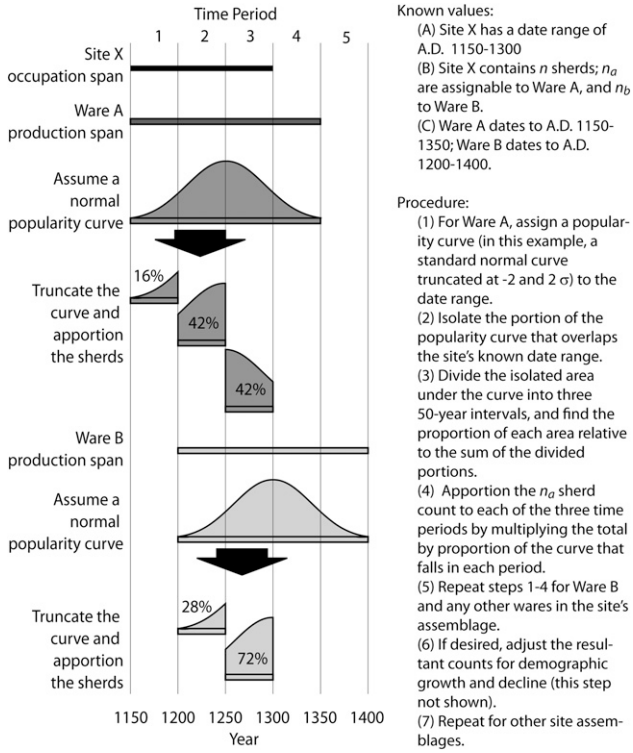

Fig. S1. Overview of the ceramic apportioning procedure. Reprinted from the *Journal of Archaeological Science* (4), Copyright 2012, with permission from Elsevier.

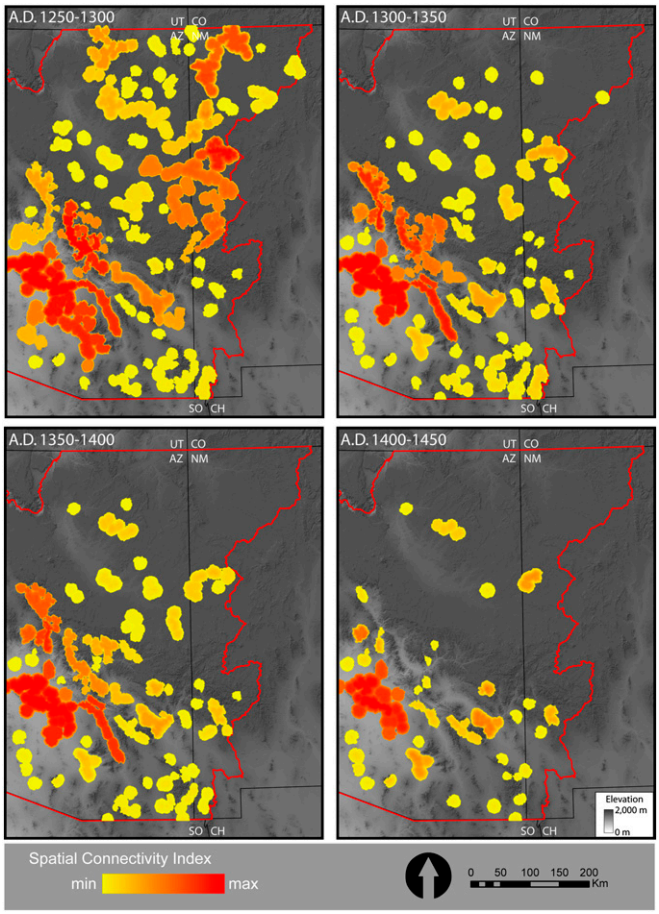

Fig. S2. Maps of the degree of spatial connectivity among settlements through time. These maps show overlapping cost-adjusted buffers (i.e., taking terrain into account) around all sites greater than 12 rooms. Sites with overlapping buffers are considered to be spatially connected. Buffers are color scaled based on the number of sites they contain. Darker colors represent portions of the study area characterized by greater spatial connectivity.

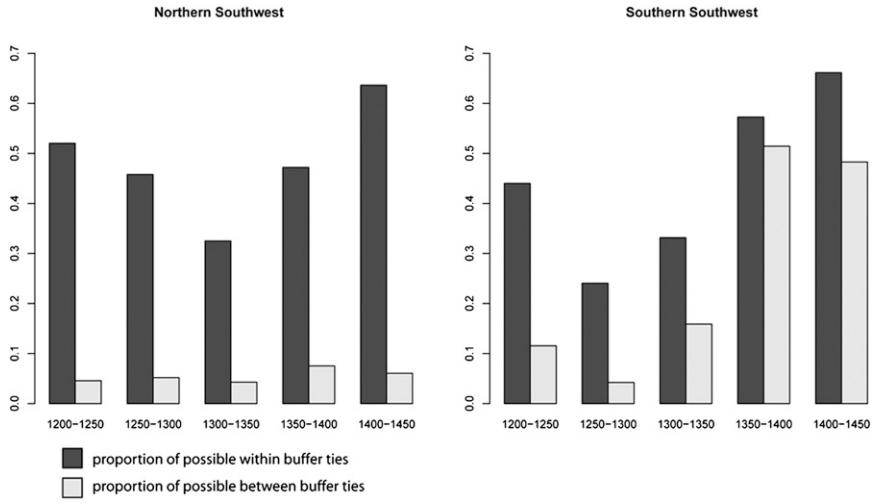

Fig. S3. Proportions of possible ties (i.e., density) among sites within overlapping 9-km cost-adjusted buffers and among sites in different buffers by time period. Ties are defined as sites with ≥0.75 similarity scores.

Table S1. All decorated ceramic wares present within systematic ceramic collections

Ware	Starting date	Ending date	Total count
Alameda Brown Ware	1065	1425	90
Babacomari Series	700	1450	4,011
Chihuahuan Series	1200	1450	1,233
Chuska White Ware	800	1300	3,712
Cibola White Ware	550	1330	175,591
Coconino Buff Ware	1050	1150	35
Dragoon Series	700	1100	465
Early White Mountain Red Ware	1000	1300	53,481
Grasshopper Ware	1330	1375	152
Hawikuh Glaze Ware	1630	1680	337
Hopi White Ware	1100	1400	472
Jeddito Orange Ware	1250	1350	1,050
Jeddito Yellow Ware	1300	1900	18,432
Jornada Mogollon Brown Ware	1000	1350	1,679
Kinishba Red Ware	1300	1400	7
Kinishba Ware	1300	1350	140
Kintiel-Klagetoh Ware	1250	1300	494
Late Middle Gila Red Ware	1300	1350	5
Late White Mountain Red Ware	1280	1425	22,396
Little Colorado White Ware	1050	1250	10,733
Lower Colorado Buff Ware	800	1900	4,276
Matsaki Buff Ware	1375	1680	2,704
Maverick Mountain Series	1265	1450	2,995
Mesa Verde White Ware	575	1300	67,885
Middle Gila Buff Ware and Gray Ware	300	1450	128,589
Mimbres White Ware	850	1150	4,395
Mogollon Brown Ware	775	1400	7,933
Navajo Painted Ware	1750	1950	1
Prescott Gray Ware	1000	1425	8,091
Puerco Valley Red Ware	1030	1200	3,727
Rio Grande Glaze Ware	1313	1700	1
Rio Grande White Ware	1050	1545	232
Roosevelt Red Ware	1275	1450	121,266
Salado Series	1150	1450	2,049
San Carlos Brown Ware	1250	1450	2,055
San Francisco Mountain Gray Ware	700	1100	218
San Juan Red Ware	700	1050	532
San Simon Series	650	1200	1,852
Sichomovi Red Ware	1900	1950	2
Tizon Brown Ware	900	1890	18
Trincheras Series	700	1450	197
Tsegi Orange Ware	1000	1300	22,200
Tucson Basin Brown Ware	700	1350	85,516
Tusayan Gray Ware	600	850	76
Tusayan White Ware	800	1300	51,332
Upper San Juan White Ware	900	1050	2
Winslow Orange Ware	1250	1400	1,797
Zuni Glaze Ware	1275	1450	22,243
Zuni Matte-Paint Ware	1680	1900	436

Table S2. Mean correlations of centrality measures and bootstrapped replicates for the A.D. 1250–1300 time period

	Sample size			Percentage of original sample removed			
Measure	10	20	30	25	50	75	90
Mean correlation for degree centrality scores	0.959	0.975	0.98	0.997	0.993	0.979	0.926
Mean correlation for eigenvector centrality scores	0.973	0.983	0.987	0.999	0.998	0.992	0.927
Mean difference in network density (%)	0.616	0.608	0.605	0.276	0.461	0.894	1.603

Sample size bootstrapping looks at mean correlations of centrality measures and network ties for bootstrapped replicates of 10, 20, and 30 sherds drawn from the original ceramic database. Percentage of original sample removed bootstrapping looks at mean correlations of centrality measures and mean difference in network density (%) for bootstrapped replicates with 25%, 50%, 75%, and 90% of sites removed at random.

Table S3. Mann–Whitney *U* statistics and associated probabilities for comparisons of ceramic similarity values within overlapping 9-km cost-adjusted buffers and between buffers

Test	1200–1250	1250–1300	1300–1350	1350–1400	1400–1450
Mann–Whitney *U* statistic	137,602,798	181,715,134	12,874,255	5,846,628	55,300
P	<0.001	<0.001	<0.001	<0.001	<0.001
Difference in means	0.58	0.48	0.34	0.38	0.32

These one-sided tests assess the probability that sites within a common buffer had higher ceramic similarity scores than sites not in the same buffer. Note that the differences in mean similarity for relations among sites within and between buffers generally decline through time.

Table S4. Site ubiquities and artifact frequencies by obsidian source in the study area

Obsidian source	Site ubiquity*	Artifact frequency
Major sources		
Mule Creek	72	654
San Fran Volcanics	62	2,209
Cow Canyon	55	327
Superior	26	348
Sauceda	25	669
Jemez	20	109
Mt Floyd	14	37
Los Vidrios	13	128
Vulture	12	169
Mt Taylor	9	21
Gwynn Canyon	6	33
Tank Mountains	5	6
Red Hill	4	7
Topaz	4	5
Sand Tanks	2	7
Antelope	2	3
Los Sitios	2	2
Bull Creek	1	1
Total count		4,735

Major sources are the most frequently recovered sources from the study area and form the basis of the quantitative analyses presented here.
*The number of sites in which a particular source is present regardless of quantity.

Table S5. Frequencies of sourced obsidian artifacts by site

Site name	Site designation	Sourced obsidian artifacts
111 Ranch	AZ BB:6:73	16
3-Up	LA 150373 (NM)	33
Adobe Hill	AZ BB:1:32	14
Anderson Canyon Fort	NA 39909 (MNA)	119
Apache Creek Pueblo	LA 2949(NM)	4
Artifact Hill	AZ BB:1:55	4
Ash Terrace	AZ BB:2:19	42
Atsinna	NM G:15:1	1
None	AZ BB:3:22	1
None	AZ CC:1:3	3
None	AZ CC:2:185	1
None	AZ CC:2:23(BLM)	1
Aztec Ruins	LA 45(NM)	21
Baby Canyon Site	NA 12556 (MNA)	33
Bajada Site	AZ BB:1:6	8
Bass Point Mound	AZ U:8:23	24
Bayless Ruin	AZ BB:11:2	12
Big Bell	AZ BB:6:2	6
Cactus Forest	AZ AA:3:214	74
Camp Village	AZ BB:6:5	2
Casa Buena	AZ T:12:37	12
Casa Grande	AZ AA:2:17	134
Casa Malpais	AZ Q:15:3	4
Chavez Pass Pueblo	AZ O:4:2	96
Chevelon Ruin	AZ P:2:1	73
Cienega	NM G:15:6	8
Cline Terrace Mound	AZ U:4:33	118
Cluff Ranch	AZ CC:1:111/112	1
Crary Site	AZ CC:1:53	5
Crescent Site	AZ BB:8:6	4
Crismon	AZ U:9:173	23
Curtis Ruin(Buena Vista)	AZ CC:2:3	19
Danson 481	Danson 481 (Danson)	3
Davis Ranch Site	AZ BB:11:36	47
Dewester Site	AZ CC:1:56	1
Dinwiddie	NM S:14:1	8
Dudleyville Mound	AZ BB:2:83	3
Eagle Pass	AZ BB:4:1	1
Earven Flat Site	AZ CC:2:5	5
El Polvoron	AZ U:15:59	23
Elden Pueblo	AZ I:14:2	34
Elliott Site	AZ BB:11:27	35
Escalante	AZ U:15:3	29
Fischer site	AZ CC:2:100	4
Flieger	AZ BB:2:7	53
Foote Canyon Pueblo	AZ W:8:16	18
Fornholt	LA 164471 (NM)	20
Fort Grant Pueblo	AZ CC:5:1	5
Fort Grant Silo Site	AZ CC:5:3(AF)	1
Fourmile Ruin	AZ P:12:4	154
Gila Pueblo	AZ V:9:52	103
Granary Row	AZ U:3:299	4
Grand Canal	AZ T:12:256	26
Grapevine Canyon	AZ CC:5:5(AF)	19
Grapevine Pueblo	NA 2803 (MNA)	292
Grasshopper	AZ P:14:1	3
Haby Ranch	AZ BB:3:16	4
Heshotauthla	NM G:14:7	2
Higgins Flat	LA 8682 (NM)	3
High Mesa	AZ BB:7:5	12
Homol'ovi I	AZ J:14:3	104
Homol'ovi II	AZ J:14:15	56
Hooper Ranch Pueblo	AZ Q:15:6	12

Table S5. Cont.

Site name	Site designation	Sourced obsidian artifacts
Horse Camp Mill	Danson 616 (Danson)	4
Howard	NA 14252 (MNA)	2
Hoyapi	AZ J:6:1	23
Jose Solas Ruin	AZ BB:11:91	12
Kinnikinick	NA 1629 (MNA)	511
Las Acequias	AZ U:9:214	17
Las Colinas	AZ T:12:10	94
Las Fosas	AZ U:15:19	19
Las Tortugas	AZ U:3:297	8
Leaverton	AZ BB:6:11	15
Lippencott South Site	AZ CC:2:102	1
Lippincott North Site	AZ CC:2:104	1
Los Hermanos	AZ U:3:5	6
Los Morteros	AZ AA:12:57	50
Lost Mound	AZ BB:2:3	33
Marana Mound	AZ AA:12:251	214
Mercer Ruin	AZ O:14:1	2
Middle of the Road Site	AZ U:3:276	1
Mirabal	LA 426 (MNA)	13
Murphy Site–Safford East	AZ CC:2:103	1
Murphy Site–Safford West	AZ CC:1:52	4
None	NA 10067 (MNA)	3
None	NA 10070 (MNA)	1
None	NA 13317 (MNA)	1
New Caves	NA 486 (MNA)	13
Old Shongopavi I	NA 86 (MNA)	19
Owens-Colvin	AZ CC:1:19	2
P Ranch Canyon site	AZ CC:6:89 (BLM)	1
Pentagon Site	AZ BB:3:18	1
Pinedale Ruin	AZ P:12:2	8
Pinto Point Mound	AZ V:5:66	32
Piper Springs	AZ BB:1:34	4
Point of Pines Ruin	AZ W:10:50	161
Pollack Ruin	NA 4317 (MNA)	16
Pottery Point Ruin	AZ V:1:166	1
Pueblo de los Muertos	LA 1585 (NM)	7
Pueblo Grande	AZ U:9:1	325
Pueblo La Plata	NA 11648 (MNA)	60
Pueblo Pato	NA 11434 (MNA)	46
Pueblo Salado	AZ T:12:47	211
Pueblo Viejo	AZ T:12:73	1
Puerco Ruin	AZ Q:1:22	12
Rabid Ruin	AZ AA:12:46	27
Rattlesnake House I & II	NA 11439/11490 (MNA)	7
Rattlesnake Point	AZ Q:11:118	17
Reeve Ruin	AZ BB:11:26	44
Richardson Orchard	AZ CC:6:33(BLM)	1
Richinbar Site (B)	AZ N:16:6	30
Ridge Ruin	NA 1785 (MNA)	4
Salmon Ruins	LA 8846 (NA)	45
Schoolhouse Point Mound	AZ U:8:24	232
Scribe S	NM:12:G3:4 (ZAP)	10
Sharon Site	AZ CC:2:101	2
Sherwood Ranch	AZ Q:11:48	43
Shumway Ruin	AZ P:12:6	10
Spear Ranch	AZ CC:1:11	3
Spier 170	Spier 170 (Spier)	2
Stone Axe Ruin	AZ Q:2:22	12
Swingle's Sample	AZ BB:1:22	23
Table Rock Pueblo	AZ Q:7:5	1
Techado Spring	LA 2148 (NM)	5
Tinaja	NM G:16:1	2

Table S5. Cont.

Site name	Site designation	Sourced obsidian artifacts
TJ Ruin	LA 54955 (NM)	51
Tonto Cliff Dwellings	AZ U:8:47/48	22
Tri-R	?	3
Tsukovi	?	58
Turkey Hill Pueblo	NA 660 (MNA)	36
University Indian Ruins	AZ BB:9:3	56
Wallace Tank Ruin	AZ Q:1:199	20
Wes Jernigan Site	AZ CC:1:38	1
Whiptail Ruin	AZ BB:10:3	3
Whitmer	AZ CC:2:69	3
Wooten-Claridge Terrace Site	AZ BB:3:19	1
Wright	AZ BB:2:51	14
WS Ranch	LA 3099 (NM)	3
Yuma Wash-Safford	AZ CC:2:16	1
Yuma Wash-Tucson	AZ AA:12:122	57
Total		4,805

All site numbers are Arizona State Museum unless otherwise noted. AF, Amerind Foundation; BLM, Bureau of Land Management; MNA, Museum of Northern Arizona; NM, New Mexico; ZAP, Zuni Archaeological Program.

Table S6. Comparisons of ceramic similarity scores for sites that share and do not share an overrepresentation of a specific obsidian source

Overrepresented obsidian source	Mean ceramic similarity among sites sharing source overrepresentation	Mean ceramic similarities among all other sites with obsidian	Mann–Whitney test probability
A.D. 1200–1250			
Mule Creek Obsidian	0.314	0.292	0.913
Cow Canyon	0.263	0.155	0.884
Jemez*	0.35	0.208	0.019
San Francisco Volcanics	—	—	—
Sauceda	—	—	—
A.D. 1250–1300			
Mule Creek Obsidian	0.292	0.227	0.695
Cow Canyon	0.303	0.15	0.937
Jemez*	0.415	0.143	<0.001
San Francisco Volcanics	—	—	—
Sauceda	—	—	—
A.D. 1300–1350			
Mule Creek Obsidian*	0.397	0.235	<0.001
Cow Canyon*	0.66	0.299	<0.001
Jemez*	0.404	0.134	<0.001
San Francisco Volcanics	0.261	0.221	0.077
Sauceda*	0.341	0.127	<0.001
A.D. 1350–1400			
Mule Creek Obsidian*	0.603	0.379	<0.001
Cow Canyon*	0.911	0.484	<0.001
Jemez*	0.376	0.152	0.0247
San Francisco Volcanics	0.324	0.351	0.5871
Sauceda*	0.477	0.358	0.0244

Comparisons for the San Francisco Volcanics and Sauceda sources are not possible before A.D. 1300 because of small sample sizes. The A.D. 1400–1450 interval is also excluded because of low sample sizes.

*Overrepresented sources with significantly higher ceramic similarity than the site sample in general ($\alpha = 0.05$).